VOLUME 12 NOMOR 2 DECEMBER 2025 ISSN 2548 – 611X

JURNAL
BIOTEKNOLOGI & BIOSAINS INDONESIA

Homepage Jurnal: http://ejournal.brin.go.id/JBBI/index

UNVEILING THE ANTIDIABETIC POTENTIAL OF KEMUNING LEAVES (*Murraya paniculata* L. Jack): AN IN-SILICO EXPLORATION OF DPP-4 INHIBITORY ACTIVITY

Studi In Silico Aktivitas Antidiabetes Daun Kemuning (Murraya paniculata L. Jack) melalui Mekanisme Inhibisi DPP-4

Arif Ladika Wiratama, Taurisma Aulia Nanda, Farsya Hidayah, Anditri Weningtyas*
Department of Medicine, Faculty of Medicine, University State of Malang,
Jl. Semarang No. 5, Malang, Jawa Timur 65145
*Email: Anditri.weningtyas.fk@um.ac.id

ABSTRACT
Type 2 diabetes mellitus is a global health issue associated with insulin resistance and impaired glucose metabolism. Murraya paniculata L. Jack (kemuning) has shown antidiabetic potential, yet its role as a DPP-4 inhibitor remains underexplored. This study aimed to investigate the potential of kemuning leaf bioactive compounds as natural DPP-4 inhibitors through an in-silico approach. Compound structures were obtained from the PubChem database and analyzed using AutoDock Vina for molecular docking against the DPP-4 protein. Pharmacokinetic properties, toxicity, and drug-likeness were evaluated using pkCSM and SwissADME, while complex stability was assessed through molecular dynamics simulation (RMSF). The results showed that most compounds demonstrated favorable binding affinities (−6.8 to −7.9 kcal/mol), along with acceptable pharmacokinetic and toxicity profiles. Among the tested compounds, 1-aminoindan-1,5-dicarboxylic acid emerged as the most promising candidate for natural DPP-4 inhibition.

Keywords: *Anti-diabetic, ADMET, DPP-4, Molecular docking, Murraya paniculata*

ABSTRAK
Diabetes mellitus tipe 2 merupakan masalah kesehatan global yang terkait dengan resistensi insulin dan gangguan metabolisme glukosa. Daun Murraya paniculata L. Jack (kemuning) mengandung alkaloid dan flavonoid yang berpotensi berinteraksi dengan situs aktif DPP-4, sehingga menarik untuk dieksplorasi sebagai sumber inhibitor alami. Meskipun kemuning diketahui memiliki potensi antidiabetes, perannya sebagai inhibitor DPP-4 belum banyak diteliti. Studi ini bertujuan mengeksplorasi potensi senyawa aktif daun kemuning sebagai inhibitor DPP-4 melalui pendekatan in silico. Struktur senyawa diperoleh dari basis data PubChem dan dianalisis menggunakan AutoDock Vina untuk docking molekular terhadap protein DPP-4. Evaluasi farmakokinetik, toksisitas, dan sifat menyerupai obat dilakukan menggunakan pkCSM dan SwissADME, sedangkan stabilitas kompleks dianalisis melalui simulasi dinamika molekular (RMSF). Hasil menunjukkan sebagian besar senyawa memiliki afinitas ikatan yang baik (−6,8 hingga −7,9 kcal/mol) serta profil farmakokinetik dan toksisitas yang mendukung. Senyawa 1-Aminoindan-1,5-dikarboksilat diidentifikasi sebagai kandidat paling potensial sebagai inhibitor DPP-4 alami.

Kata Kunci: *Anti-diabetic, ADMET, DPP-4, Molecular docking, Murraya paniculata.*

Received: *20 July 2025* ***Accepted***: *4 November 2025* ***Published***: *15 December 2025*

INTRODUCTION

Diabetes is a chronic condition characterized by persistently high blood glucose levels due to problems in insulin function. These problems may occur because the body does not produce enough insulin, the insulin does not work effectively, or both factors happen together (Antar et al. 2023). Diabetes has become a serious global health issue as its prevalence continues to rise. This growing number of cases is also linked to an increased risk of severe complications such as limb amputation, loss of vision, kidney failure, and cardiovascular diseases (Zhou et al. 2024). Recent research suggests that more than 240 million people around the world may have diabetes without being diagnosed, with type 2 diabetes being the most widespread form (Hossain et al. 2024). By the year 2030, the global prevalence of type 2 diabetes is expected to reach approximately 7.079 cases per 100.000 people (Khan et al. 2020). Indonesia is predicted to be among the ten countries with the highest prevalence of type 2 diabetes, affecting around 10.8 percent of its population (Soeatmadji et al. 2023).

Type 2 diabetes (T2DM) is the most widespread form of diabetes, marked by the body's reduced sensitivity to insulin, disrupted glucose metabolism, and beta-cell dysfunction (Galicia-Garcia et al. 2020). One of the key underlying mechanisms in type 2 diabetes is the increased activity of the enzyme dipeptidyl peptidase 4 (DPP-4), which degrades incretin hormones. This process leads to lower insulin secretion and higher blood sugar levels. DPP-4 specifically contributes to the breakdown of glucagon-like peptide 1 (GLP-1) and glucose-dependent insulinotropic polypeptide (GIP), two important incretin hormones that help regulate blood glucose levels (Samyor et al. 2022). Inhibiting DPP-4 has become a recognized therapeutic approach for managing type 2 diabetes, with several synthetic drugs such as sitagliptin and vildagliptin already in use (Saini et al. 2023; Elbarbary et al. 2024). However, synthetic DPP-4 inhibitors still present certain challenges, including potential side effects and relatively high treatment costs. To address these concerns, alternative therapeutic strategies are being explored, including the use of natural compounds as a potentially safer and more affordable source of DPP-4 inhibitors.

Natural DPP-4 inhibitors from medicinal plants are increasingly explored as safer and more affordable antidiabetic agents. One such plant is the kemuning leaf (Murraya paniculata L. Jack), traditionally used to manage various health conditions, including metabolic disorders (Menezes et al. 2017). Kemuning leaves contain diverse bioactive compounds, including flavonoids, tannins, steroids or triterpenoids, essential oils, and coumarins, which exhibit anti-inflammatory and antidiabetic activities (Farida et al. 2021).

Although previous in silico studies have demonstrated the antidiabetic potential of kemuning compounds via targets such as α-glucosidase and GLUT4 (Arifianti 2016; Hamdi 2024), no studies have yet investigated its potential as a DPP-4 inhibitor. Targeting DPP-4 is particularly promising because DPP-4 degrades incretin hormones (GLP-1 and GIP), which regulate insulin secretion and glucagon levels in a glucose-dependent manner, reducing the risk of hypoglycemia and improving glycemic control (Epelde 2024). Molecular docking provides a reliable in silico approach to predict interactions between bioactive compounds and target proteins, offering preliminary insights before in vitro and in vivo experiments (Chang et al., 2022). Building on this gap, the present study aims to examine the potential of active compounds from kemuning leaves as DPP-4 inhibitors using molecular docking analysis, contributing to the development of natural and safe antidiabetic agents.

MATERIALS AND METHODS

Research Settings and Period

This research was conducted entirely in silico at the Molecular Biology Laboratory, Faculty of Mathematics and Natural Sciences, Universitas Negeri Malang. All computational analyses, including molecular docking, molecular dynamics simulations, and ADMET profiling, were performed using bioinformatics software and tools available in the laboratory. The study was conducted in July 2025.

Materials

Bioactive phytochemical compounds derived from *Murraya paniculata* L. Jack (kemuning leaves) were used in this study, selected based on previous findings reported by Odion et al. (2024). These compounds were cross-referenced and retrieved from the PubChem database in three-dimensional (SDF) format. The structure of the target protein, dipeptidyl peptidase-4 (DPP-4), was obtained from the Protein Data Bank (PDB ID: 5Y7H) and was determined using X-ray diffraction at a resolution of 3.0 Å. Prior to molecular docking, the protein was prepared by removing water molecules, adding polar hydrogens, and assigning Gasteiger charges using AutoDockTools to ensure correct geometry and protonation states.

Several bioinformatics tools were used to perform the analyses. Molecular docking was carried out using AutoDock Vina, while visualization of protein–ligand interactions was performed with PyMOL. Pharmacokinetic, drug-likeness, and toxicity predictions were assessed using SwissADME and pkCSM web servers. To evaluate the stability and flexibility of the protein–ligand complexes, molecular dynamics simulations were conducted focusing on Root Mean Square Fluctuation (RMSF) analysis. Five compounds with the lowest docking scores were selected for this analysis. The selected ligands were retrieved from the PubChem database (PubChem IDs provided in Table 1) and screened based on their binding affinity to DPP-4. Additional tools, such as Discovery Studio Visualizer, were used for further interaction analysis when necessary.

Methods

Selection of Bioactive Compounds

Bioactive compounds from kemuning leaves (*Murraya paniculata* L. Jack) were selected based on phytochemical profiling reported by Odion et al. (2024). The identified compounds were then validated through the PubChem database (https://pubchem.ncbi.nlm.nih.gov/) to ensure the accuracy of their chemical structures. The three-dimensional (3D) structures of these compounds were downloaded from PubChem in structure data file (SDF) format for use in the molecular docking process.

Prediction of ADMET Properties

The pharmacokinetic and toxicity profiles of bioactive compounds from kemuning leaves (*Murraya paniculata* L. Jack) were evaluated using ADMET analysis to predict their drug-likeness, safety, and potential effectiveness as DPP-4 inhibitors. The ADMET prediction was performed using the pkCSM web-based platform (https://biosig.lab.uq.edu.au/pkcsm/), which analyzes chemical structures inputted in SMILES format to estimate various pharmacokinetic parameters (Pires et al., 2015). In addition to ADMET profiling, drug-likeness evaluation was conducted using the SwissADME web tool (http://www.swissadme.ch/). This analysis focused on evaluating drug-likeness parameters based on established filters, including Lipinski's Rule of Five, Ghose filter, Veber criteria, Egan filter, and Muegge filter. The combined results from pkCSM and SwissADME were integrated to comprehensively evaluate the suitability of the selected compounds as potential oral antidiabetic agents targeting DPP-4.

Toxicity Prediction

In addition to pharmacokinetic analysis, toxicity prediction was carried out using the Protox 3.0 platform (https://tox.charite.de/protox3/) to comprehensively assess the safety profile of each selected compound. This evaluation included the prediction of toxicity class and median lethal dose (LD50) values, which was used to estimate acute oral toxicity, along with potential toxic effects on specific organs and systems such as the liver (hepatotoxicity), nervous system (neurotoxicity), kidneys (nephrotoxicity), respiratory system (respiratory toxicity), and cardiovascular system (cardiotoxicity). Furthermore, the analysis covered risks related to carcinogenicity, immunotoxicity, mutagenicity, and cytotoxicity. The results of this toxicity assessment served as a basis for identifying compounds with favorable safety characteristics, supporting their potential as natural DPP-4 inhibitor candidates (Banerjee et al. 2024).

Target Protein and Ligand Preparation

The three-dimensional structure of the DPP-4 enzyme was obtained from the Protein Data Bank (https://www.rcsb.org/) with PDB ID: 5Y7H. This structure was selected because it represents a high-resolution human DPP-4 co-crystallized with a known inhibitor, providing a reliable template for molecular docking studies. The protein structure was prepared by removing water molecules, ligands, and other non-essential chains using Discovery Studio Visualizer 2021 Client (Dassault Systèmes, Massachusetts, USA). Following the removal of water molecules and non-essential ligands, the protein structure was reprocessed and saved in .PDB format to be used in subsequent molecular docking simulations. For the ligands, the three-dimensional structures of the selected bioactive compounds were converted into PDBQT format using Open Babel in PyRx 8.0 (The Scripps Research Institute, Florida, USA), followed by energy minimization. This procedure was performed to ensure that each ligand adopted its most stable, low-energy conformation prior to molecular docking, as initial two-dimensional representations do not accurately reflect energetically favorable three-dimensional structures. (Fadlan and Nusantoro 2021).

Molecular Docking

Molecular docking was performed using AutoDock Vina integrated within the PyRx 8.0 platform (The Scripps Research Institute, Florida, USA). The active site of the DPP-4 enzyme was determined based on previous studies by Guanga Ortizo et al. (2025). The DPP-IV structure is composed of two propeller domains, each containing a cavity of approximately 35–40 Å, forming two accessible openings identified as the enzyme's active sites, which include hydrophobic S1 and charged S2 pockets. Specific residues, including His126, Glu205, Glu206, Val207, Ser209, Phe357, Arg358, Tyr547, Trp629, Ser630, Tyr631, Tyr666, and Asn710, have been reported to interact with commercial DPP-IV inhibitors, with the catalytic triad (His740, Asp708, and Ser630) considered critical for effective inhibition. The docking grid was centered at X: 59.5654, Y: 55.3636, Z: 71.5460, with dimensions of X: 41.2454, Y: 31.3926, and Z: 62.5794, and was selected to encompass all catalytic residues within the binding pocket.

Root Mean Square Fluctuation (RMSF) Analysis

To further analyze complex stability after docking, the protein and ligand structures obtained from the docking results were merged into a single complex using PyMOL software ver. 3.1 (DeLano Scientific LLC, Palo Alto, CA, USA) and saved in PDB format. The merged complex was then uploaded to the CABS-flex 3.0 web server (https://lcbio.pl/cabsflex3/) for simulation using default parameters. RMSF analysis was selected to evaluate the local flexibility of the protein-ligand complex and to identify stable binding regions. RMSF values for each residue were obtained to assess the flexibility and stability of the complex, with particular focus on the active site region (Wróblewski et al. 2025).

Data Analysis

The docking results were analyzed by evaluating binding affinity values and by observing the types of interactions, including hydrogen bonds and hydrophobic interactions, formed between the ligands and target protein residues. Visualization of these interactions was performed using Discovery Studio Visualizer. The outcomes of ADMET, drug-likeness, and toxicity evaluations were presented in tables and heatmaps generated using GraphPad Prism version 10.1.2. RMSF analysis results were visualized using a scatter plot illustrating the fluctuation values of each amino acid residue within the protein-ligand complex.

RESULTS AND DISCUSSION

Bioactive Compound in *Murraya paniculata* L Jack.

Previous study by (Odion et al. 2024) performed a metabolite profiling of semi-polar secondary metabolites from the methanol extract of kemuning leaves (*Murraya paniculata* L. Jack) using GC-MS and HPLC chromatography. The chromatographic analysis identified 16 secondary metabolites, including compounds from the alkaloid,

flavonoid, tannin, glycoside, triterpenoid, and steroid classes. However, no saponin compounds were detected in the methanol extract according to their analysis. To validate the identified compounds, a cross-check was performed using the PubChem database. Out of the 16 compounds, two could not be found using a name-based search: Pyrano[2,3-b]indole, 2,3,4,4a,9,9a-hexahydro-4a-methyl- (C6) and trans-2,3-Methylenedioxy-β-methyl-β-nitrostyrene (C13). The molecular formulas of these two compounds, C12H15NO for C6 and C11H11NO4 for C13, were then used to perform an alternative search, which identified N-Benzyl-4-piperidone (C6) and 1-Aminoindan-1,5-dicarboxylic acid (C13) as suitable substitutes. These two compounds were selected to replace the original unlisted compounds in subsequent analyses, as presented in Table 1.

Table 1. List of bioactive compounds identified from the methanol extract of kemuning leaves (*Murraya paniculata* L. Jack) based on the study by Odion et al. (2024) including substitute compounds obtained through PubChem cross-checking.

Compound Code	Compound Name	Molecular Formula	Molecular Weight
C1	2-Methoxy-4-vinylphenol	C9H10O2	150.17
C2	Dimethyl 6-methoxyquinolinate	C10H11NO5	225.20
C3	Estran-17-one, 3-hydroxy	C18C28O2	276.42
C4	1-(3',5'-Dibromo-4'-hydroxyphenyl)	C11H7NO3Br4	341.18
C5	Pyridazin-3(2H)-one, 5-chloro-2-(3-	C12H8N2O2F3	269.19
C6	N-Benzyl-4-piperidone	C12H15NO	189.25
C7	Pyrazine, 2,5-dimethyl-3-(3-methyl-	C16H25N2	245.41
C8	Isoquinoline, 6,7,8-trimethoxy-	C12H13NO3	219.24
C9	Isoquinoline, 3,4-dihydro-6,7	C12H15NO2	205.27
C10	7-Methyl-1,2-dihydroquinoxalin-2-	C9H8N2O	160.17
C11	2-1-Phenyl ethylidene-hydrazono-3-	C16H15N3S	281.40
C12	6-Methyl-triazolo(4,3-b)(1,2,4)-	C4H5N5	123.09
C13	1-Aminoindan-1,5-dicarboxylic acid	C11H11NO4	221.22
C14	2-Nitro-4-(trifluoromethyl)phenol	C7H4F3NO3	207.11
C15	Ethanimidamide, 2-chloro-N2-(2-	C8H8Cl2N2O3S	283.13
C16	Perhydro-htx-2-one, 2-depentyl-	C16H27NO3	281.39

Pharmacokinetic, Toxicity, and Drug-Likeness Evaluation

Pharmacokinetic, drug-likeness, and toxicity analyses were conducted to assess the drugability of bioactive compounds derived from *Murraya paniculata* L. Jack as potential DPP-4 inhibitors. The evaluation of physicochemical properties using pkCSM revealed that most of the selected compounds met the acceptable criteria for oral drug candidates, with molecular weights under 500 g/mol, hydrogen bond donors (HBD) less than 5, acceptors (HBA) below 10, and TPSA values under 140 Å². These parameters suggest good membrane permeability and favorable oral bioavailability (Figure 1). Compounds such as Dimethyl 6-methoxyquinolinate and Pyridazin-3(2H)-one, 5-chloro-2-(3-...) even showed TPSA below 80 Å², which may support better blood–brain barrier (BBB) permeability. LogP values ranging between 1–5 further support balanced lipophilicity, aiding both solubility and permeability.

In the drug-likeness screening using Lipinski, Ghose, Veber, Egan, and Muegge rules, most compounds showed no violations (Figure 2). Only one compound, 6-Methyl-triazolo(4,3-b)(1,2,4)-, exhibited three violations in the Ghose filter, suggesting reduced oral potential. Toxicity profiling via pkCSM revealed that the majority of compounds were non-mutagenic, non-hepatotoxic, and exhibited low cardiotoxic and immunotoxic potential (Figure 3). However, 2-Methoxy-4-vinylphenol and 1-(3′,5′-Dibromo-4′-hydroxyphenyl) showed higher predicted risks for skin sensitization and hepatotoxicity. Despite these findings, all compounds fell into toxicity classes 3 to 5,

indicating general safety when administered orally according to the OECD classification system (Figure 4) (Banerjee et al. 2024). The heatmap visualization of toxicity risk further affirmed that most compounds carried low to moderate toxicity probability scores.

These in silico pharmacokinetic and toxicity predictions strongly support the therapeutic potential of *Murraya paniculata* compounds as safe and effective DPP-4 inhibitor candidates. This is in line with previous in vivo studies which demonstrated the antidiabetic properties of kemuning leaves. Prior research showed that the infusion of *M. paniculata* leaves could significantly lower blood glucose levels in hyperglycemic mice, primarily due to the action of flavonoids that modulate carbohydrate metabolism, improve glucose uptake, and enhance insulin secretion (Handayani and Maharani 2019). Moreover, administration of the extract at doses of 100–400 mg/kg over 14 to 21 days led to notable reductions in glucose, cholesterol, triglycerides, and lipid profiles in diabetic rats, while simultaneously enhancing antioxidant enzyme activities such as SOD, CAT, and GPx (Gautam et al. 2012). These findings collectively reinforce the pharmacological relevance of kemuning-derived compounds and justify further investigation of their bioactivity through both computational and experimental approaches.

No.	Property	Descriptor	Compound														
			C1	C2	C3	C4	C5	C6	C7	C8	C9	C10	C11	C12	C13	C14	C15	C16
1	MW	g/mol	150.18	225.2	276.4	521.78	304.65	189.26	246.4	219.24	241.72	160.2	281.384	135.13	221.2	207.11	283.1	281.4
2	LogP	g/mol	2.04	0.66	3.56	3.45	2.91	1.85	4.19	2.26	-2.84	1.23	3.56	-0.17	0.56	2.31	1.55	2.94
3	#Rot.Bonds	g/mol	2	3	0	1	2	2	6	3	2	0	2	0	2	1	4	4
4	#HBA	g/mol	2	6	2	3	4	2	2	4	2	2	4	5	3	3	4	3
5	#HBD	g/mol	1	0	1	2	0	0	0	0	1	1	0	0	3	1	1	1
6	TPSA	Å	65.744	92.139	121.876	141.783	115.91	84.537	111.56	93.768	101.89	69.08	121.096	56.73	91.5	75.74	102.9	121.19
7	Absorption	Solubility (mol/L)	-1.958	-1.63	-4.608	-4.819	-3.861	-1.496	-3.696	-2.505	-0.172	-1.78	-4.591	-0.909	-2.892	-3.026	-2.553	-3.456
8	Absorption	Caco2 permeability	1.499	0.939	1.598	0.869	1.392	1.724	1.218	1.766	1.766	1.226	1.553	1.287	-0.091	0.883	0.706	1.321
9	Absorption	Intestinal (%)	91.965	97.039	95.451	86.311	94.277	94.79	94.415	97.941	88.055	85.69	95.051	97.367	38.12	88.634	90.9	93.655
10	Absorption	Skin permeability	-2.262	-2.659	-3.077	-2.921	-2.722	-2.131	-2.574	-2.375	-2.732	-2.75	-2.226	-2.479	-2.735	-2.504	-2.581	-3.324
11	Absorption	P-glycoprotein substrate	No	No	No	No	No	No	No	No	No	No	Yes	No	No	No	No	No
12	Absorption	P-glycoprotein I inhibitor	No	No	Yes	No	No	No	No	No	No	No	No	No	No	No	No	No
13	Absorption	P-glycoprotein II inhibitor	No	No	No	No	No	No	No	No	No	No	Yes	No	No	No	No	No
14	Distribution	VDss (human)	0.118	-0.626	0.475	-0.261	-0.374	0.818	0.385	-0.288	0.381	-0.15	0.181	-0.599	-0.429	-0.123	-0.441	0.126
15	Distribution	Fraction unbound	0.322	0.511	0.156	0.231	0.171	0.429	0.204	0.274	0.606	0.388	0.072	0.512	0.482	0.268	0.381	0.409
16	Distribution	BBB permeability	0.289	-0.713	0.343	-0.752	0.456	0.332	0.333	0.151	0.035	-0.25	0.179	-0.331	-0.604	-0.096	-0.875	-0.075
17	Distribution	CNS permeability	-2.042	-2.965	-2.259	-2.073	-1.643	-1.982	-2.411	-2.464	-2.077	-2.22	-1.205	-2.983	-2.823	-2.101	-2.956	2.908
18	Metabolism	CYP2D6 substrate	No	No	No	No	No	No	No	No	Yes	No	No	No	No	No	No	No
19	Metabolism	CYP3A4 substrate	No	No	Yes	Yes	Yes	No	No	No	Yes	No	Yes	No	No	No	No	No
20	Metabolism	CYP1A2 inhibitor	Yes	No	No	No	Yes	No	No	Yes	No	Yes	Yes	No	No	Yes	No	No
21	Metabolism	CYP2C19 inhibitor	No	No	No	Yes	Yes	No	Yes	Yes	No	No	Yes	No	No	No	No	No
22	Metabolism	CYP2C9 inhibitor	No	No	No	No	No	No	No	No	No	No	No	No	No	No	No	No
23	Metabolism	CYP2D6 inhibitor	No	No	No	No	No	No	No	No	No	No	No	No	No	No	No	No
24	Metabolism	CYP3A4 inhibitor	No	No	No	No	No	No	No	No	No	No	No	No	No	No	No	No
25	Excretion	Total clearance log mL/min/kg)	0.233	0.936	0.936	-0.231	0.312	1.047	1.534	0.668	1.662	0.616	0.203	0.65	0.371	0.445	0.186	1.324
26	Excretion	Renal OCT2 substrate	No	No	Yes	No	No	No	No	No	Yes	No	No	No	No	No	No	No
27	Toxicity	AMES toxicity	Yes	No	No	No	No	No	No	No	No	No	No	No	No	Yes	Yes	No
28	Toxicity	Max. tolerated dose (human) (log mg/kg/day)	1.067	1.434	-0.333	0.109	0.553	0.174	1.162	0.732	-0.053	0.574	0.178	1.216	0.495	0.882	0.898	0.058
29	Toxicity	hERG I inhibitor	No	No	No	No	No	No	No	No	No	No	No	No	No	No	No	No
30	Toxicity	hERG II inhibitor	No	No	Yes	No	No	No	No	No	No	No	No	No	No	No	No	No
31	Toxicity	Oral Rat Acute Toxicity (LD50) (mol/kg)	2.076	2.953	1.745	2.554	2.768	2.454	1.955	2.474	1.867	2.063	1.913	2.672	2.467	2.517	2.497	2.317
32	Toxicity	Oral Rat Chronic Toxicity (LOAEL) (log mg/kg_bw/day)	2.019	2.244	1.943	1.192	0.554	1.422	2.119	1.939	1.724	1.418	0.417	0.593	1.872	1.586	2.393	1.638
33	Toxicity	Hepatotoxicity	No	Yes	No	No	Yes	No	No	No	No	No	No	No	No	No	No	No
34	Toxicity	Skin Sensitization	Yes	No	Yes	No	No	Yes	Yes	No	No	No	No	No	No	Yes	No	No
35	Toxicity	T. pyriformis toxicity (µg/L)	0.071	0.147	1.061	0,877	0.607	0.777	0.773	0.568	0.241	0.211	1.785	0.268	0.285	1.609	0.96	0.882
36	Toxicity	Minnow toxicity	1.957	2.45	0.451	0.873	0.767	0.973	-0.146	1.403	2.409	1.952	-0.508	1.141	2.547	1.306	0.806	1.416

Figure 1. ADMET evaluation results of selected bioactive compounds from *Murraya paniculata* L. Jack based on pkCSM predictions.

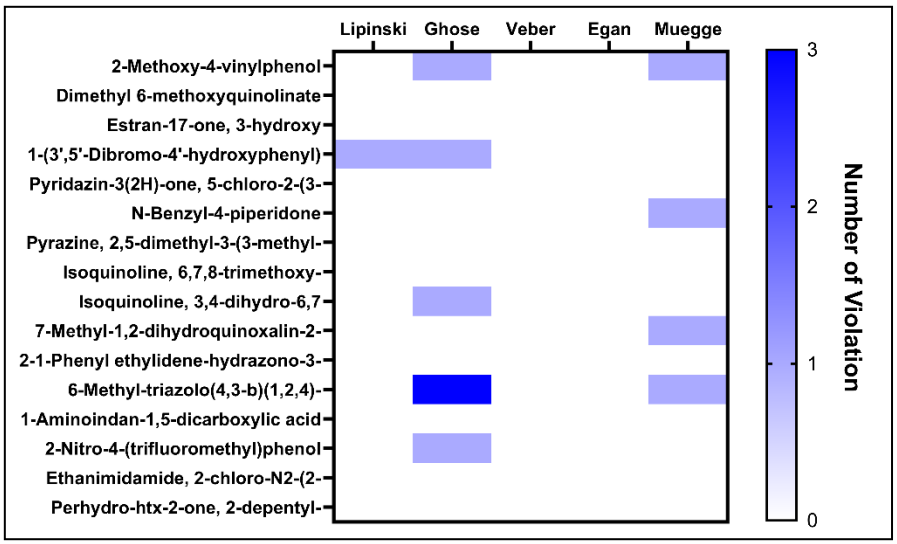

Figure 2. Drug-likeness profiling results of bioactive compounds from kemuning leaves (*Murraya paniculata* L. Jack) based on Lipinski, Ghose, Veber, Egan, and Muegge criteria

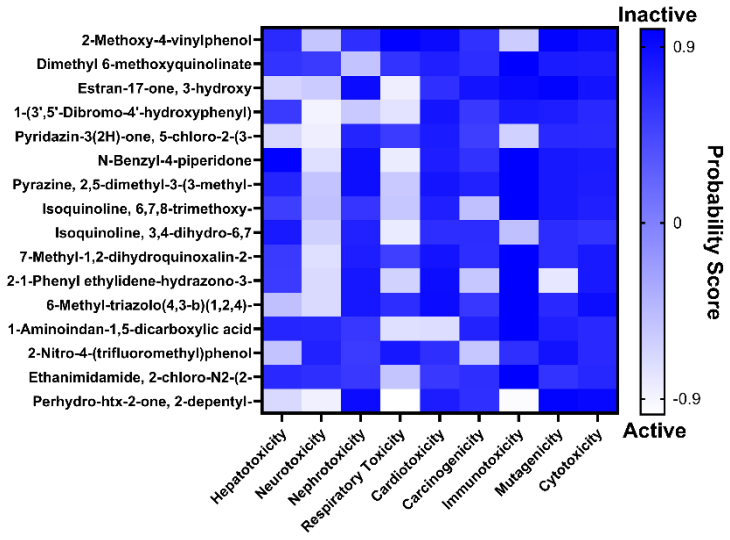

Figure 3. Prediction results of bioactive compounds from *Murraya paniculata* L Jack ADMET using pKCSM webserver

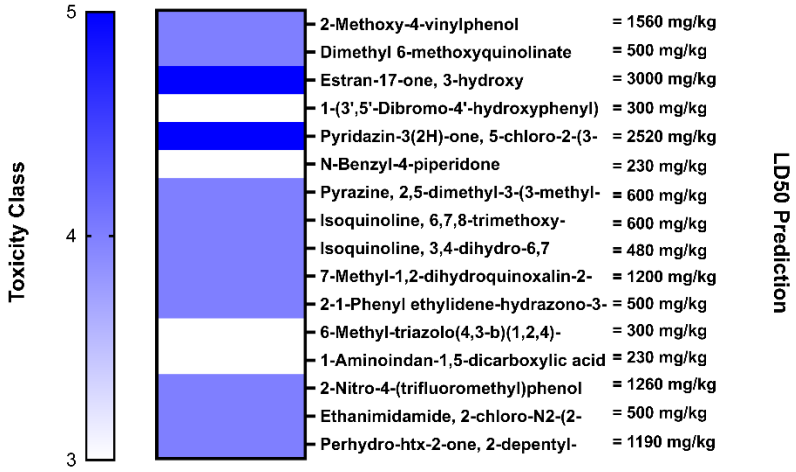

Figure 4. toxicity profiles of bioactive compounds from *Murraya paniculata* L Jack.

Molecular Docking Results

Molecular docking analysis was conducted to predict the binding affinity and interaction profiles of selected bioactive compounds from kemuning leaves (*Murraya paniculata* L. Jack) against the DPP-4 enzyme (Table 2). The docking results showed binding affinities ranging from −6.8 kcal/mol to −7.9 kcal/mol, while the reference compound Sitagliptin exhibited a binding affinity of −8.2 kcal/mol (Figure 3). Among the tested ligands, Estran-17-one, 3-hydroxy displayed the highest binding affinity at −7.9 kcal/mol, followed by Ethanimidamide, 2-chloro-N2-(2-... at −7.7 kcal/mol and 2,4-1-Phenyl ethylidene-hydrazono at −7.1 kcal/mol. Other compounds, such as 1-Aminoindan-1,5-dicarboxylic acid and Pyridazin-3(2H)-one, 5-chloro-2-(3-...), showed slightly lower binding affinities of −6.9 kcal/mol and −6.8 kcal/mol, respectively. The visualization of docking poses revealed that the ligands occupied the DPP-4 binding pocket, which consists of the hydrophobic S1 pocket (Chain A, colored cyan) and the charged S2 pocket (Chain B, colored magenta) (Table 2). The ligands were observed to form key interactions with active site residues, including His126, Glu205, Glu206, Val207, Ser209, Phe357, Arg358, Tyr547, Trp629, Ser630, Tyr631, Tyr666, and Asn710, as well as the catalytic triad residues His740, Asp708, and Ser630 that are essential for DPP-4 inhibition.

Table 2. Binding affinity values and key residue interactions of selected bioactive compounds from Murraya paniculata L Jack. Against DPP-4 based on molecular docking analysis. Bolded residues indicate key similarities with the active site of DPP-4.

Ligand	Binding Affinity (kcal/mol)	Position of Chemical Interaction	
		Hydrogen Bond	Hydrophobic Interaction
Sitagliptin	-8.2	Arg125, **Ser209**, **Tyr547**, Tyr585, **Ser630**, Tyr662, **Asn710**	Glu206, **Phe357**, **Tyr666**
Estran-17-one, 3-hydroxy	-7.9	-	**Phe357**
Ethanimidamide, 2-chloro-N2-(2-…)	-7.7	Ser237, Ser239	Tyr238, Tyr241, Phe713
2-1-Phenyl ethylidene-hydrazono	-7.1	Gln123	Lys122, Trp124, Phe240, Val252, Ala707, Asp739
1-Aminoindan-1,5-dicarboxylic acid	-6.9	**Ser209, Tyr547, Ser630,** Tyr662	Arg125, **Glu205, Phe357, Tyr666**
Pyridazin-3(2H)-one, 5-chloro-2-(3-…)	-6.8	Gln123	Phe240, Val252

The interaction profiles of each ligand against the DPP-4 enzyme revealed distinct patterns involving key active site residues. The control ligand, Sitagliptin (−8.2 kcal/mol), demonstrated strong interactions with essential residues including Ser209, Phe357, Arg358, Tyr547, Ser630, Tyr631, Tyr666, and Asn710 which are known to play important roles in DPP-4 inhibition. The interactions shown in sitagliptin are dominated by hydrogen bonds, which indicate the very strong inhibitory potential of this drug. Among the tested bioactive compounds, Estran-17-one, 3-hydroxy (−7.9 kcal/mol) showed strong binding through interactions with Glu205, Glu206, Ser209, Phe357, Tyr547, and Tyr666. The interactions shown in this compound are dominated by Van der Waals interactions. Ethanimidamide, 2-chloro-N2-(2-…) (−7.7 kcal/mol) it does not form significant interactions with key active site residues, and its binding pose indicates that the compound is positioned between the S1 and S2 pockets. It only exhibits interaction with one key residue, Asp708, through Van der Waals interaction.

2-1-Phenyl ethylidene-hydrazono (−7.1 kcal/mol) also showed no interactions with key residues, but this compound managed to form several strong interactions through Pi- interactions such as Pi-Cation,

Pi-Anion, and Pi-Pi-Stacked as well as several Alkyl and Pi-Alkyl interactions. 1-Aminoindan-1,5-dicarboxylic acid (−6.9 kcal/mol) showed some interaction with Glu206, Val207, Ser209, Phe357, Tyr547, Ser630, and Tyr666 with this compound is also predominantly stabilized by hydrogen bonds. Lastly, Pyridazin-3(2H)-one, 5-chloro-2-(3-…) (−6.8 kcal/mol) exhibited interactions with Glu206, Ser209, Tyr547, Ser630, and Tyr666, aligning with several key residues involved in DPP-4 inhibition. These findings suggest that multiple bioactive compounds from *Murraya paniculata* L. Jack share similar binding behavior with Sitagliptin, reinforcing their potential as DPP-4 inhibitory candidates.

Molecular Docking Results

Molecular docking analysis was conducted to predict the binding affinity and interaction profiles of selected bioactive compounds from kemuning leaves (*Murraya paniculata* L. Jack) against the DPP-4 enzyme (Table 2). The docking results showed binding affinities ranging from −6.8 kcal/mol to −7.9 kcal/mol, while the reference compound Sitagliptin exhibited a binding affinity of −8.2 kcal/mol (Figure 3). Among the tested ligands, Estran-17-one, 3-hydroxy displayed the highest binding affinity at −7.9 kcal/mol, followed by Ethanimidamide, 2-chloro-N2-(2-... at −7.7 kcal/mol and 2,4-1-Phenyl ethylidene-hydrazono at −7.1 kcal/mol. Other compounds, such as 1-Aminoindan-1,5-dicarboxylic acid and Pyridazin-3(2H)-one, 5-chloro-2-(3-...), showed slightly lower binding affinities of −6.9 kcal/mol and −6.8 kcal/mol, respectively. The visualization of docking poses revealed that the ligands occupied the DPP-4 binding pocket, which consists of the hydrophobic S1 pocket (Chain A, colored cyan) and the charged S2 pocket (Chain B, colored magenta) (Table 2). The ligands were observed to form key interactions with active site residues, including His126, Glu205, Glu206, Val207, Ser209, Phe357, Arg358, Tyr547, Trp629, Ser630, Tyr631, Tyr666, and Asn710, as well as the catalytic triad residues His740, Asp708, and Ser630 that are essential for DPP-4 inhibition (Figure 5).

The interaction profiles of each ligand against the DPP-4 enzyme revealed distinct patterns involving key active site residues. The control ligand, Sitagliptin (−8.2 kcal/mol), demonstrated strong interactions with essential residues including Ser209, Phe357, Arg358, Tyr547, Ser630, Tyr631, Tyr666, and Asn710 which are known to play important roles in DPP-4 inhibition. The interactions shown in sitagliptin are dominated by hydrogen bonds, which indicate the very strong inhibitory potential of this drug. Among the tested bioactive compounds, Estran-17-one, 3-hydroxy (−7.9 kcal/mol) showed strong binding through interactions with Glu205, Glu206, Ser209, Phe357, Tyr547, and Tyr666. The interactions shown in this compound are dominated by Van der Waals interactions. Ethanimidamide, 2-chloro-N2-(2-…) (−7.7 kcal/mol) it does not form significant interactions with key active site residues, and its binding pose indicates that the compound is positioned between the S1 and S2 pockets. It only exhibits interaction with one key residue, Asp708, through Van der Waals interaction.

2-1-Phenyl ethylidene-hydrazono (−7.1 kcal/mol) also showed no interactions with key residues, but this compound managed to form several strong interactions through Pi- interactions such as Pi-Cation, Pi-Anion, and Pi-Pi-Stacked as well as several Alkyl and Pi-Alkyl interactions. 1-Aminoindan-1,5-dicarboxylic acid (−6.9 kcal/mol) showed some interaction with Glu206, Val207, Ser209, Phe357, Tyr547, Ser630, and Tyr666 with this compound is also predominantly stabilized by hydrogen bonds. Lastly, Pyridazin-3(2H)-one, 5-chloro-2-(3-…) (−6.8 kcal/mol) exhibited interactions with Glu206, Ser209, Tyr547, Ser630, and Tyr666, aligning with several key residues involved in DPP-4 inhibition. These findings suggest that multiple bioactive compounds from *Murraya paniculata* L. Jack share similar binding behavior with Sitagliptin, reinforcing their potential as DPP-4 inhibitory candidates.

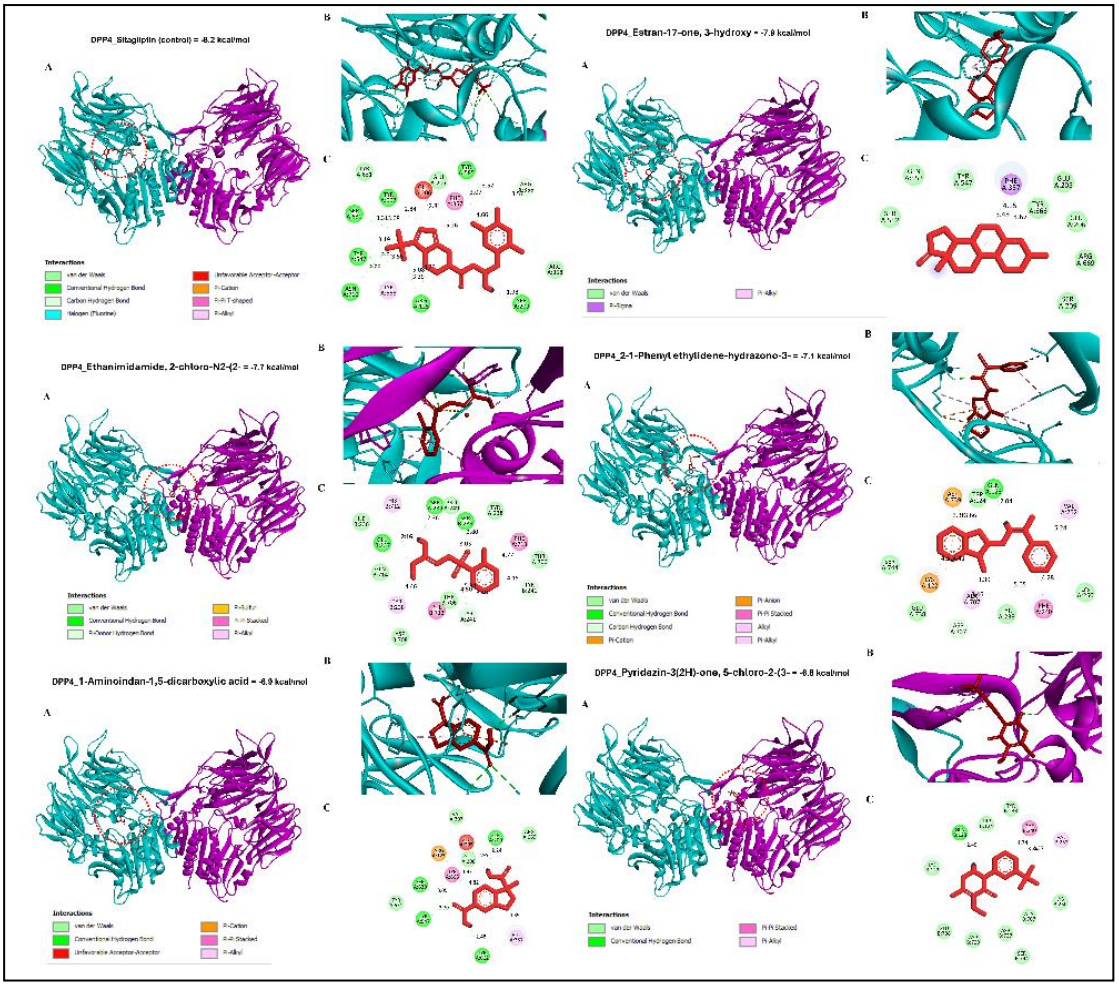

Figure 5. Molecular docking visualization of selected bioactive compounds from *Murraya paniculata* L. Jack. against DPP-4. (A) Interaction site location within S1 and S2 pockets, (B) Ligand binding pose, (C) 2D interaction diagram showing bonds with DPP-4 residues.

These findings support the therapeutic potential of kemuning-derived phytochemicals as natural DPP-4 inhibitors. The relatively strong binding affinities and shared interaction patterns with sitagliptin reinforce their candidacy. This aligns with growing interest in DPP-4 inhibition as a treatment approach for type 2 diabetes mellitus (T2DM), a condition that continues to rise globally (Epelde 2024). DPP-4 inhibitors act by preserving incretin hormones (GLP-1, GIP), thereby enhancing insulin secretion and glycemic control (Naim 2024). Their ability to manage blood glucose without triggering hypoglycemia or weight gain has made them a cornerstone in diabetes care (Komamine et al. 2019; Liu et al. 2020).

However, despite their efficacy, synthetic DPP-4 inhibitors such as sitagliptin and vildagliptin are not without drawbacks, including reports of fever, gastrointestinal disturbances, and eye irritation (Zhou et al. 2019). This underlines the importance of exploring safer alternatives, particularly from natural products with lower toxicity profiles. In this context, the tested compounds, especially Estran-17-one, 3-hydroxy and 1-Aminoindan-1,5-dicarboxylic acid show exhibited interaction profiles comparable to sitagliptin, making them promising leads for further experimental validation. Their natural origin, favorable binding behavior, and potential to avoid adverse effects present a compelling case for developing *Murraya paniculata*-based antidiabetic therapies.

Molecular Dynamics Simulation: RMSF Analysis

The Root Mean Square Fluctuation (RMSF) analysis was conducted to assess the flexibility and stability of DPP-4 residues when interacting with selected bioactive

compounds from *Murraya paniculata* L. Jack, compared with Sitagliptin as the reference inhibitor. The RMSF profiles showed that all ligand–DPP-4 complexes presented fluctuating patterns along the residue sequence, reflecting the dynamic behavior of the protein structure during the simulation. Sitagliptin as the control demonstrated relatively moderate residue fluctuations, with RMSF values generally maintained below 4.5 Å, indicating stable interactions and limited flexibility (Figure 6). Estran-17-one, 3-hydroxy displayed the highest fluctuations among all tested ligands, with peaks reaching approximately 7 Å, suggesting increased structural flexibility that may influence its binding stability. Ethanimidamide, 2-chloro-N2-(2-...) exhibited local peaks particularly around residue number 300, while the overall RMSF values remained below 6 Å, indicating moderate structural flexibility. In contrast, 2-1-Phenyl ethylidene-hydrazono and 1-Aminoindan-1,5-dicarboxylic acid showed relatively stable fluctuation patterns, comparable to Sitagliptin, with RMSF values predominantly below 4.5 Å, suggesting good complex stability. Pyridazin-3(2H)-one, 5-chloro-2-(3-...) demonstrated balanced fluctuations, with RMSF values peaking around 5–6 Å. These findings indicate that although all ligand–DPP-4 complexes maintained structural integrity during the simulation, the degree of flexibility varied depending on the ligand, where ligands such as 2-1-Phenyl ethylidene-hydrazono and 1-Aminoindan-1,5-dicarboxylic acid displayed fluctuation profiles closest to the control, supporting their potential as stable DPP-4 inhibitor candidates.

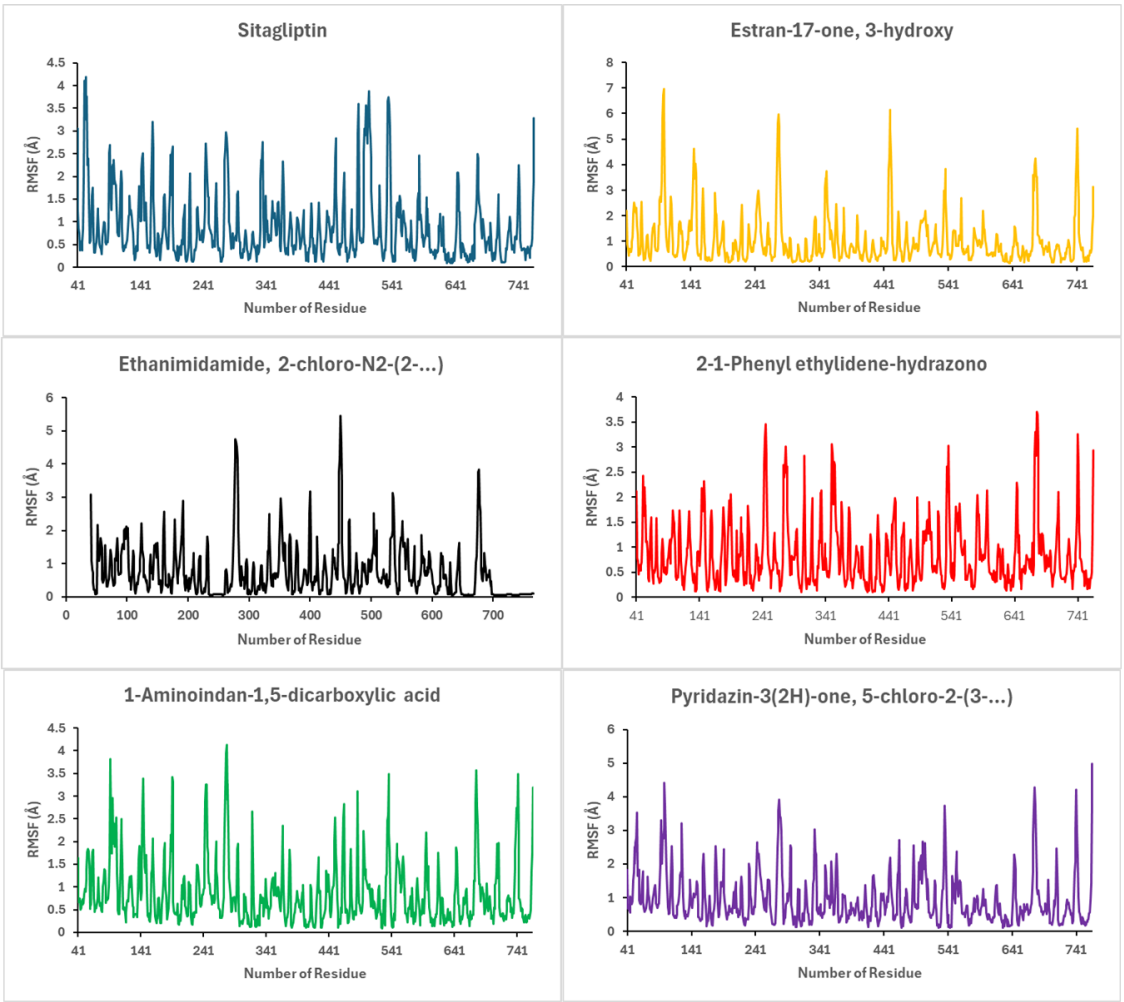

Figure 6. RMSF (Root Mean Square Fluctuation) plot of DPP-4 protein in complex with selected ligand. The fluctuations of amino acid residues indicate the flexibility and stability of the protein-ligand complex over the simulation time. Lower RMSF values represent more stable binding regions, particularly at the active site.

This study, through comprehensive *in-silico* analysis, identified several bioactive compounds from kemuning leaves with promising potential as natural DPP-4 inhibitors. Among these, 1-Aminoindan-1,5-dicarboxylic acid emerged as the most favorable candidate compared to the standard drug Sitagliptin. Although its binding affinity is moderate, this compound interacts precisely at critical residues essential for DPP-4 inhibition, underscoring its potential effectiveness. This finding is further supported by molecular dynamics analysis, which showed stable residue fluctuations through RMSF evaluation, indicating that the compound does not induce increased flexibility or instability at the DPP-4 active site. These findings suggest that *Murraya paniculata L. Jack* holds strong potential as a source of plant-based antidiabetic agents. With further validation through laboratory and clinical studies, its bioactive constituents could contribute to the development of safer, affordable, and effective therapies for managing type 2 diabetes.

CONCLUSION

Based on the comprehensive in silico evaluation, 1-Aminoindan-1,5-dicarboxylic acid was identified as the most promising bioactive compound from *Murraya paniculata* L. Jack, showing strong binding affinity, critical interactions with key DPP-4 residues, favorable pharmacokinetic and drug-likeness profiles, and stable complex formation comparable to Sitagliptin. These results highlight its potential to effectively inhibit DPP-4 activity, suggesting a direct biological impact on incretin-mediated glucose regulation. Therefore, this compound represents a strong candidate for development as a natural antidiabetic agent and should be prioritized for experimental validation in both in vitro and in vivo models to confirm efficacy and safety.

ACKNOWLEDGEMENTS

The authors would like to express their sincere gratitude to the Institute for Research and Community Service (LPPM) Universitas Negeri Malang for supporting this research through internal funding under contract number 24.2.872/UN32.14.1/LT/2025.

REFERENCES

Antar SA, Ashour NA, Sharaky M, Khattab M, Ashour NA, Zaid RT, Roh EJ, Elkamhawy A, Al-Karmalawy AA (2023) Diabetes mellitus: Classification, mediators, and complications; A gate to identify potential targets for the development of new effective treatments. Biomedicine & Pharmacotherapy 168:115734. https://doi.org/10.1016/j.biopha.2023.115734

Arifianti AA (2016) Uji Aktivitas Anti-Diabetes dan Antioksidan Ekstrak Daun Kemuning (Murraya paniculata): Metode Penghambatan α-Glukosidase dan DPPH In Vitro. Skripsi, Universitas Negeri Jember

Banerjee P, Kemmler E, Dunkel M, Preissner R (2024) ProTox 3.0: a webserver for the prediction of toxicity of chemicals. Nucleic Acids Research 52:W513–W520. https://doi.org/10.1093/nar/gkae303

Elbarbary NS, Ismail EA, El-Hamamsy MH, Ibrahim MZ, Elkholy AA (2024) The DPP-4 inhibitor sitagliptin improves glycaemic control and early-stage diabetic nephropathy in adolescents with type 1 diabetes using the MiniMed 780G advanced hybrid closed-loop system: a randomised controlled trial. Diabetologia 67:2637–2649. https://doi.org/10.1007/s00125-024-06265-7

Epelde F (2024) Transforming Diabetes Care: The Expanding Role of DPP-4 Inhibitors in Cardiovascular and Renal Protection. Medicina 60:1793. https://doi.org/10.3390/medicina60111793

Fadlan A, Nusantoro YR (2021) The Effect of Energy Minimization on The Molecular Docking of Acetone-Based Oxindole Derivatives. JKPK 6:69. https://doi.org/10.20961/jkpk.v6i1.45467

Farida Y, Qodriah R, Widyana AP, Zauhara Ifani (2021) Uji Aktivitas Antioksidan, Uji Antikolesterol dan Toksisitas dari Ekstrak Etanol Daun Kemuning. Maj Farmasetika 6:24–31. https://doi.org/10.24198/mfarmasetika.v6i0.

Galicia-Garcia U, Benito-Vicente A, Jebari S, Larrea-Sebal A, Siddiqi H, Uribe KB, Ostolaza H, Martín C (2020) Pathophysiology of Type 2 Diabetes Mellitus. IJMS 21:6275. https://doi.org/10.3390/ijms21176275

Gautam M, Gupta A, Vijaykumar M, Rao C, Goel R (2012) Studies on the hypoglycemic effects of Murraya paniculata Linn. extract on alloxan-induced oxidative stress in diabetic and non-diabetic models. Asian Pacific Journal of Tropical Disease 2:S186–S191. https://doi.org/10.1016/s2222-1808(12)60149-2

Guanga Ortizo RG, Sharma V, Tsai M-L, Nargotra P, Sun P-P, Chen CW, Dong C-D (2025) Integrating in silico, in vitro, and in situ approaches for characterization of novel peptides from tilapia (Oreochromis niloticus) viscera hydrolysates with dipeptidyl-peptidase IV inhibitory activity. Food Bioscience 63:105619. https://doi.org/10.1016/j.fbio.2024.105619

Hamdi R (2024) Studi In sillico Antidiabetes Senyawa Golongan Flavonoid Kemuning (Murraya paniculata L.) Terhadap PPAR-γ dan Glucose Transporter-4. Skripsi, UIN Syarif Hidayatullah

Handayani SR, Maharani PT (2019) Uji Aktivitas Antidiabetes Infusa Daun Kemuning (Murraya Paniculata L Jack.) Pada Mencit Putih Jantan Yang Diinduksi Glukosa. Indonesian Journal On Medical Science 6:86–90.

Hossain MdJ, Al-Mamun Md, Islam MdR (2024) Diabetes mellitus, the fastest growing global public health concern: Early detection should be focused. Health Science Reports 7. https://doi.org/10.1002/hsr2.2004

Khan MAB, Hashim MJ, King JK, Govender RD, Mustafa H, Al Kaabi J (2020) Epidemiology of Type 2 Diabetes - Global Burden of Disease and Forecasted Trends. J Epidemiol Glob Health 10:107–111. https://doi.org/10.2991/jegh.k.191028.001

Komamine M, Kajiyama K, Ishiguro C, Uyama Y (2019) Cardiovascular risks associated with dipeptidyl peptidase-4 inhibitors monotherapy compared with other antidiabetes drugs in the Japanese population: A nationwide cohort study. Pharmacoepidemiology and Drug 28:1166–1174. https://doi.org/10.1002/pds.4847

Liu H, Guo L, Xing J, Li P, Sang H, Hu X, Du Y, Zhao L, Song R, Gu H (2020) The protective role of DPP4 inhibitors in atherosclerosis. Eur J Pharmacol 875:173037. https://doi.org/10.1016/j.ejphar.2020.173037

Menezes CDA, De Oliveira Garcia FA, De Barros Viana GS, Pinheiro PG, Felipe CFB, De Albuquerque TR, Moreira AC, Santos ES, Cavalcante MR, Garcia TR, Silva TF, Coutinho HDM, De Menezes IRA (2017) Murraya paniculata (L.) (Orange Jasmine): Potential Nutraceuticals with Ameliorative Effect in Alloxan-Induced Diabetic Rats. Phytotherapy Research 31:1747–1756. https://doi.org/10.1002/ptr.5903

Naim MohdJ (2024) A Review of Dipeptidyl Peptidase-4 (DPP-4) and its potential synthetic derivatives in the management of Diabetes Mellitus. J Angiotherapy 8. https://doi.org/10.25163/angiotherapy.819417

Odion EE, Ambe DA, Akhere M, Odiete EC (2024) Profiling of Semi-polar Secondary Metabolites from the Methanol Leaf of Murraya paniculata (L.) Jack by Chromatographic Technique. Nigerian Journal of Pharmaceutical and Biomedical Research 8:1–10

Pires DEV, Blundell TL, Ascher DB (2015) pkCSM: Predicting Small-Molecule Pharmacokinetic and Toxicity Properties Using Graph-Based Signatures. J Med Chem 58:4066–4072. https://doi.org/10.1021/acs.jmedchem.5b00104

Saini K, Sharma S, Khan Y (2023) DPP-4 inhibitors for treating T2DM - hype or hope? an analysis based on the current literature. Front Mol Biosci 10:1130625. https://doi.org/10.3389/fmolb.2023.1130625

Samyor D, Calderwood D, Carey M, Das AB, Green BD, Deka SC (2022) Dipeptidyl peptidase-4 (DPP-4) inhibitory activity and glucagon-like peptide (GLP-1) secretion in arsenically safe pigmented red rice (Oryza sativa L.) and its product. J Food Sci Technol 59:4016–4024. https://doi.org/10.1007/s13197-022-05444-x

Soeatmadji DW, Rosandi R, Saraswati MR, Sibarani RP, Tarigan WO (2023) Clinicodemographic Profile and Outcomes of Type 2 Diabetes Mellitus in the Indonesian Cohort of DISCOVER: A 3-Year Prospective Cohort Study. JAFES 38:68–74. https://doi.org/10.15605/jafes.038.01.10

Wróblewski K, Zalewski M, Kuriata A, Kmiecik S (2025) CABS-flex 3.0: an online tool for simulating protein structural flexibility and peptide modeling. Nucleic Acids Research 53:W95–W101. https://doi.org/10.1093/nar/gkaf412

Zhou B, Rayner AW, Gregg EW, Sheffer KE, Carrillo-Larco RM, Bennett JE. (2024) Worldwide trends in diabetes prevalence and treatment from 1990 to 2022: a pooled analysis of 1108 population-representative studies with 141 million participants. The Lancet 404:2077–2093. https://doi.org/10.1016/s0140-6736(24)02317-1

Zhou X-J, Ding L, Liu J-X, Su L-Q, Dong J-J, Liao L (2019) Efficacy and short-term side effects of sitagliptin, vildagliptin and saxagliptin in Chinese diabetes: a randomized clinical trial. Endocr Connect 8:318–325. https://doi.org/10.1530/EC-18-0523